Quantum Chaos and the Hydrogen Atom in Strong Magnetic Fields

D. Delande and J.-C. Gay

Laboratoire de Spectroscopie Hertzienne de l'ENS,
Tour 12, Etage 1, 4 Place Jussieu, F-75252 Paris Cedex 05, France

We study the classical and quantum dynamics of the hydrogen atom in a strong magnetic field. At low field, approximate dynamical symmetries exist, allowing a complete description of the system. As the magnetic field is increased, the classical dynamics smoothly evolves from regular to chaotic. However, the dynamical symmetries are not completely destroyed. There are "scars" of these symmetries which manifest in the energy spectrum and eigenstates. They also imply a partial phase-space localization of the quantum motion. In the experimental spectra, these scars are responsible for the modulations known as "Quasi-Landau" resonances.

1. THE HYDROGEN ATOM IN A MAGNETIC FIELD. EQUIVALENCE WITH A SYSTEM OF COUPLED OSCILLATORS

The hydrogen atom in a strong magnetic field is one of the simplest chaotic system. The classical and quantum dynamics can be studied (see sections 2,3,4), and stimulating experimental results have been obtained [1-4]. Conjectures on quantum chaos, established on model systems or observed on nuclear energy levels [5-8], can be tested on a "real" completely calculable system.

The hamiltonian of the hydrogen atom in a magnetic field is (in atomic units, neglecting relativistic effects and assuming an infinitely massive nucleus) :

$$H = \frac{\vec{p}^2}{2} - \frac{1}{r} + \frac{\gamma}{2} L_z + \frac{\gamma^2}{8} (x^2+y^2) \qquad (1)$$

where $\gamma = B/B_c$ is the magnetic field (along z-axis) measured in atomic units ($B_c = 2.35\ 10^5$ T). L_z (projection of the angular momentum on z-axis) and parity are constants of the motion.

In the following, we consider the $L_z = M = 0$ states (somewhat similar conclusions are obtained for the other low M series). The paramagnetic term $\gamma L_z/2$, constant over a given M series, can be disregarded.

The Hydrogen Atom Editors: G.F. Bassani · M. Inguscio · T.W. Hänsch

As the hamiltonian (1) is time-independent, the total energy is constant. If another independent constant exists, the motion is regular (number of constants = number of degrees of freedom). Otherwise, the system is chaotic.

In the *strong-field regime*, the Coulomb potential (with spherical symmetry) and the diamagnetic potential $\gamma^2(x^2+y^2)/8$ (with cylindrical symmetry) are of the same order of magnitude. Their symmetries being not compatible, no constant exists and the system turns chaotic [9][10].

As the diamagnetic interaction actually couples almost any hydrogenic state with any other one, the study of (1) is not straightforward. A structure describing the hydrogenic spectrum in its whole is convenient : the dynamical group SO(2,2) (subgroup with fixed value of M of the full dynamical group SO(4,2)) [11-14].

It is easily built using the equivalence of the hydrogen atom with a pair of harmonic oscillators. The semi-parabolic coordinates are defined through :

$$\begin{cases} \mu = \sqrt{r+z} \\ \nu = \sqrt{r-z} \end{cases} . \qquad (2)$$

In this system of coordinates, Schrödinger's equation is (E is the energy) :

$$\left\{ H(\mu) + H(\nu) + \frac{\gamma^2}{8} \mu^2\nu^2(\mu^2+\nu^2) \right\} |\psi\rangle = 4 |\psi\rangle \qquad (3)$$

with $$H(\mu) = -\frac{\partial^2}{\partial\mu^2} - \frac{1}{\mu}\frac{\partial}{\partial u} + \frac{M^2}{\mu^2} - 2E\mu^2 .$$

$H(\mu)$ is the radial part of the hamiltonian of a 2-dimensional harmonic oscillator with frequency $\sqrt{-2E}$ and angular momentum M. The dynamical group describing the radial motion of the 2-dimensional harmonic oscillator is SO(2,1), the hermitian generators of which are :

$$\begin{cases} S_1^{(\alpha)} = \frac{\alpha}{4}\left(\frac{\partial^2}{\partial\mu^2} + \frac{1}{\mu}\frac{\partial}{\partial\mu} - \frac{M^2}{\mu^2} \right) + \frac{1}{4\alpha}\mu^2 \\ S_2^{(\alpha)} = \frac{i}{2}(1 + \mu\frac{\partial}{\partial\mu}) \\ S_3^{(\alpha)} = -\frac{\alpha}{4}\left(\frac{\partial^2}{\partial\mu^2} + \frac{1}{\mu}\frac{\partial}{\partial\mu} - \frac{M^2}{\mu^2} \right) + \frac{1}{4\alpha}\mu^2 \end{cases} \qquad (4)$$

with α a positive adjustable parameter.

They satisfy the commutation relations of a SO(2,1) Lie algebra :

$$\begin{cases} [S_1^{(\alpha)}, S_2^{(\alpha)}] = -\,i\,S_3^{(\alpha)} \\ [S_2^{(\alpha)}, S_3^{(\alpha)}] = \;\;i\,S_1^{(\alpha)} \\ [S_3^{(\alpha)}, S_1^{(\alpha)}] = \;\;i\,S_2^{(\alpha)} \;. \end{cases} \tag{5}$$

Upon choosing $\alpha = 1/\sqrt{-2E}$, $S_3^{(\alpha)}$ is proportional to the hamiltonian $H(\mu)$. The eigenvalues of $S_3^{(\alpha)}$ are $n_1+(|M|+1)/2$, labelled with the non-negative integer n_1.

The three generators of the SO(2,1) group act like the three components of the angular momentum for the usual SO(3) rotation group. $S_\pm^{(\alpha)} = S_1^{(\alpha)} \pm i\,S_2^{(\alpha)}$ are ladder operators, rising n_1 by ± 1. The matrix elements are known from group representation theory and involve simple algebraic expressions [12][14].

The dynamical group of the hydrogen atom (or of the equivalent oscillator problem) is the direct product SO(2,1) $\otimes$ SO(2,1) = SO(2,2). The six generators are the three components of $\vec{S}^{(\alpha)}$ and those of $\vec{T}^{(\alpha)}$ (the latter is defined as $\vec{S}^{(\alpha)}$ but with the change $\mu \to \nu$). Using (2) and (3), Schrödinger's equation is cast under a pure algebraic form as a function of the generators :

$$\left\{ S_3^{(\alpha)}+T_3^{(\alpha)} - \alpha + \frac{\gamma^2\alpha^4}{2}(S_3^{(\alpha)}+S_1^{(\alpha)})\,(T_3^{(\alpha)}+T_1^{(\alpha)})\,(S_3^{(\alpha)}+S_1^{(\alpha)}+T_3^{(\alpha)}+T_1^{(\alpha)}) \right\} |\psi\rangle = 0 \tag{6}$$

with $\alpha = (-2E)^{-1/2}$.

2. CLASSICAL DYNAMICS

The hydrogen atom and the equivalent system of coupled oscillators have the same classical dynamics. The latter can be studied using the dynamical coordinates $(\vec{S}^{(\alpha)}, \vec{T}^{(\alpha)})$. The hamiltonian of the system is the classical form of (6).

Another set of dynamical coordinates is the "energy-phase" coordinates for the oscillators along the μ and ν directions, defined as :

$$\begin{cases} \varphi_S = \tan^{-1}\left(S_2^{(\alpha)}/S_1^{(\alpha)}\right) = 2\,\tan^{-1}\,(p_\mu/\mu) \\ \varphi_T = \tan^{-1}\left(T_2^{(\alpha)}/T_1^{(\alpha)}\right) = 2\,\tan^{-1}\,(p_\nu/\nu) \;. \end{cases} \tag{7}$$

$(\varphi_S, \varphi_T, S_3^{(\alpha)}, T_3^{(\alpha)})$ is a set of canonical coordinates complying with the dynamical symmetries of the unperturbed system [14]. Indeed, in zero magnetic field, from (6), $S_3^{(\alpha)}$ and $T_3^{(\alpha)}$ are constant, and φ_S and φ_T are linear functions of time. This system of coordinates provides one with *the most simple description of the Kepler motion of the electron around the nucleus.*

There is a scaling law for the classical dynamics. It depends on the single parameter :

$$\beta = \frac{\gamma^2}{(-2E)^3} \qquad (8)$$

which is the ratio of the diamagnetic force to the Coulomb force.

The various sets of trajectories associated with different values of γ and E, and same value of β, are simply homothetic. The strong-field regime where chaos takes place corresponds to values of β around unity.

The equations of the motion can be numerically solved. From the calculated trajectories in the 4-dimensional phase space, we deduce Poincaré surfaces of section. In order to preserve the $\vec{S} \leftrightarrow \vec{T}$ symmetry, we use a symmetrical $\varphi_S + \varphi_T = 0$ surface of section and represent the section in the plane of canonically conjugate coordinates : $(X_3^{(\alpha)} = T_3^{(\alpha)} - S_3^{(\alpha)}$, $\Delta\varphi = (\varphi_T - \varphi_S)/2)$. These simply represent the differences of the energies and phases of the two oscillators.

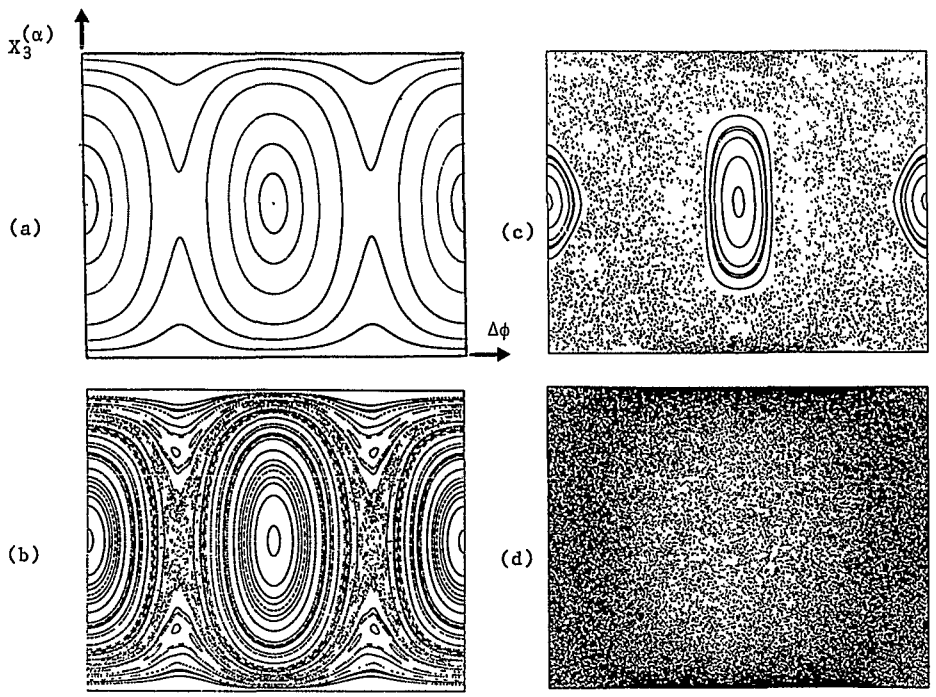

Figure 1 : Some Poincaré surfaces of section obtained in the $(-\alpha < X_3^{(\alpha)} = T_3^{(\alpha)} - S_3^{(\alpha)} < \alpha,\ -\pi < \Delta\varphi = (\varphi_T - \varphi_S)/2 < \pi)$ plane

(a) β=0.01 The motion is fully regular (see section 4)
(b) β=1 A small chaotic region appears
(c) β=5 Mixed regular-chaotic regime
(d) β=70 Fully chaotic regime

Figure 1 represents a set of Poincaré surfaces of section. At low field, the phase space trajectories are confined on 2-dimensional invariant tori, which intersect the surface of section along the 1-dimensional invariant curves of Fig. 1a. Near β=1, some invariant tori are destroyed (Fig. 1b) and chaos takes place. As the magnetic field is increased, the fraction of chaotic phase space smoothly increases (Fig. 1c). Above $\beta \simeq 60$ and up to the ionization limit ($\beta=\infty$), the whole phase space is chaotic, except for very small regions [14,15].

3. QUANTUM SPECTRUM AND EIGENSTATES

As the diamagnetic interaction mixes together all the hydrogenic states, including the continuum, understanding the quantum behaviour of the hydrogen atom in a strong magnetic field has been a challenging question for years.

An efficient way for calculating the energy spectrum and the eigenstates in the strong-field regime is to use the dynamical group SO(2,2) (see section 1) and (6). In an eigenbasis of the equivalent oscillator system (eigenstates of $S_3^{(\alpha)}$ and $T_3^{(\alpha)}$), the generators $(\vec{S}^{(\alpha)}, \vec{T}^{(\alpha)})$ connect a given $|n_1\ n_2\ M\rangle$ state to its nearest neighbors $|n_1 \pm 1\ n_2 \pm 1\ M\rangle$ only. Hence, the hamiltonian matrix (6) has few non-zero elements, and leads to efficient numerical diagonalization [15-18].

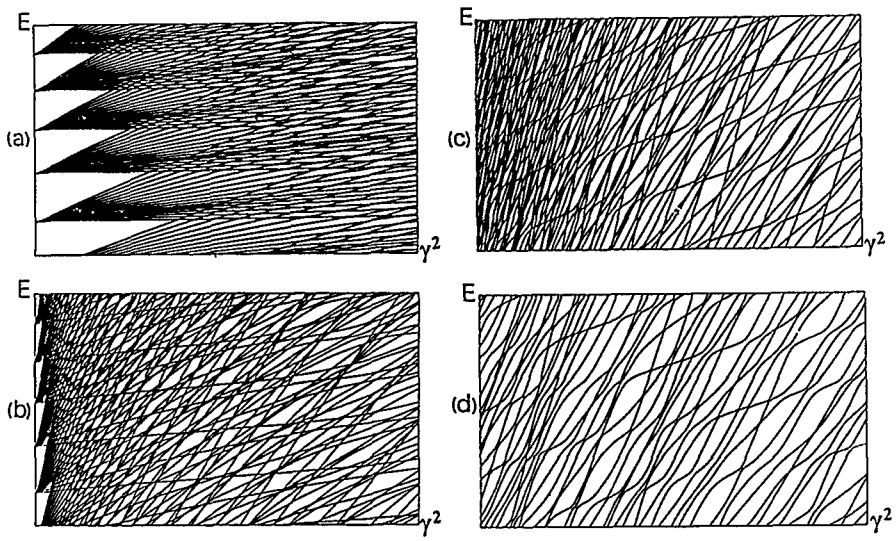

Figure 2 : Energy diagrams of the hydrogen atom as a function of γ^2 :

(a) Low field (regular) $-4\ 10^{-4} \leqslant E \leqslant -3\ 10^{-4}$; $0 \leqslant \gamma^2 \leqslant 1.4\ 10^{-10}$

(b) Moderate field (regular-chaotic) $-4\ 10^{-4} \leqslant E \leqslant -3\ 10^{-4}$; $0 \leqslant \gamma^2 \leqslant 1.4\ 10^{-9}$

(c) High field (regular-chaotic) $-4\ 10^{-4} \leqslant E \leqslant -3\ 10^{-4}$; $1\ 10^{-9} \leqslant \gamma^2 \leqslant 1.4\ 10^{-8}$

(d) High field (chaotic) $-2.5\ 10^{-4} \leqslant E \leqslant -2\ 10^{-4}$; $6\ 10^{-9} \leqslant \gamma^2 \leqslant 1.3\ 10^{-8}$

The convergency of the calculations is excellent, except very close to the ionization limit.

One of the key points for doing such calculations is to use a basis having the appropriate symmetry properties. The oscillator basis is such. Numerical diagonalization of the hamiltonian (1) in an hydrogenic basis would give very poorly converging results in the strong-field regime.

Figure 2 shows plots of the energy spectrum as a function of γ^2 (square of the magnetic field). The different plots correspond to increasing values of β, ranging from 0 (low-field limit) to about 100 (chaotic strong-field regime).

4. THE LOW-FIELD LIMIT

In the limit of vanishing magnetic field (the so-called inter-ℓ-mixing regime), the eigenstates are obtained by first order perturbation theory, that is, by diagonalizing the diamagnetic term inside a given n-manifold. The restriction of the diamagnetic perturbation to a n-manifold is then an adiabatic invariant, that is, a constant of the motion to first order in γ^2. It can be expressed as a function of the "energy-phase" coordinates (7) just by keeping in the diamagnetic term of equation (6), the part which does not change the $n = S_3^{(\alpha)} + T_3^{(\alpha)}$ value. The result is [12]:

$$1 + \Lambda = \frac{4}{n^2} S_3^{(\alpha)} T_3^{(\alpha)} \left(3 + 2 \cos(\varphi_S - \varphi_T) \right) \qquad (9)$$

with $S_3^{(\alpha)} + T_3^{(\alpha)} = n$ (principal quantum number).

This result can be reexpressed in terms of the Runge-Lenz vector $\vec{A}=\vec{p}\times\vec{L}-\vec{r}/r$ as : $\Lambda = 4\vec{A}^2 - 5A_z^2$ [19,20].

The expression of constant of the motion (9) holds both in classical and quantum mechanics. It means that, beside E and L_z, another quantity is conserved during the classical motion. Hence, the motion is regular. Moreover, the invariant tori are known analytically. This can be checked in Fig. 1a where the invariant curves are in excellent agreement with the predictions of (9).

In the quantum formalism, the eigenstates are labelled with an integer K ranging from 0 (highest state) to n-|M|-1 (lowest state). The wavefunctions are usually very complicated in real space, showing lot of oscillations and, except for few of them, no clear spatial localization.

Performing a significant comparison between the classical and quantum dynamics requires to define a distribution function in phase space rather than in real space [21,22]. The most famous one is the Wigner density, but other definitions are possible, all of them sharing the same semi-classical behaviour. In the present case, the Q-density defined from the coherent states of the

SO(2,2) dynamical group is used [14]. For each eigenstate, the distribution function depends on the 4 dynamical variables $(\varphi_s, \varphi_r, S_3^{(\alpha)}, T_3^{(\alpha)})$. We verified that, as expected from general arguments [21], it is localized near the energy surface H = E with a gaussian dispersion. A further section in the plane $\varphi_s + \varphi_r = 0$ allows us to plot it as a function of $(X_3^{(\alpha)}, \Delta\varphi)$, which is done in Fig 3 for the (n=89,K=40,M=0) state. As expected, the phase-space distribution function is localized near a classical invariant curve Λ = Cst (compare with Fig. 1a).

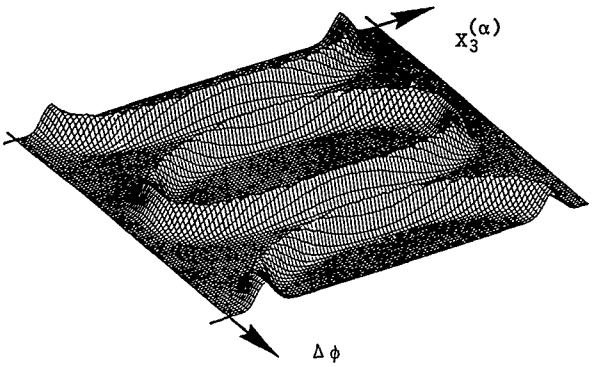

Figure 3 : Phase-space distribution function for the (n=89,K=40,M=0) state represented in the $(-\alpha < X_3^{(\alpha)} < \alpha,\ -\pi < \Delta\varphi < \pi)$ plane. It is localized near the invariant curve of the classical motion

From (9) and Fig. 1a, one easily shows that there exist two types of classical motion according to the sign of the constant Λ :

* $\Lambda > 0$ (inner invariant curves in Fig. 1a). The phase difference between the μ and ν oscillators is bounded. The motion along the invariant curve is around the central fixed point $(X_3^{(\alpha)}=0, \Delta\varphi=0)$, which corresponds to the motion of the atomic electron in the z=0 plane. The associated quantum eigenstates are the upper states of the diamagnetic manifolds (see Fig. 2a). Their symmetry is of an approximate "rotational" type [19] (However, the rotational character does not refer to a spherical property in real space [12,19]). The associated phase space distribution functions are localized near the central fixed point (see Fig. 4a).

* $\Lambda < 0$ (outer invariant curves in Fig. 1a). The phase difference between the two oscillators slowly and smoothly increases (or decreases) with time, which expresses that their correlation is weak. The invariant curves are localized near the $X_3^{(\alpha)} = \pm\alpha$ axis. The associated quantum eigenstates have an approximate "vibrational" symmetry [19]. They are the lower states of each diamagnetic manifold. The phase-space distribution functions are localized near the invariant curves (see Fig. 4b).

The $\Lambda = 0$ invariant curve is a separatrix between the two types of motion. Its quantum counterpart is visible in Fig. 2a : near the separatrix, the period

of the classical motion tends to infinity ("critical slowing down"), and the spacing between consecutive diamagnetic components dramatically decreases.

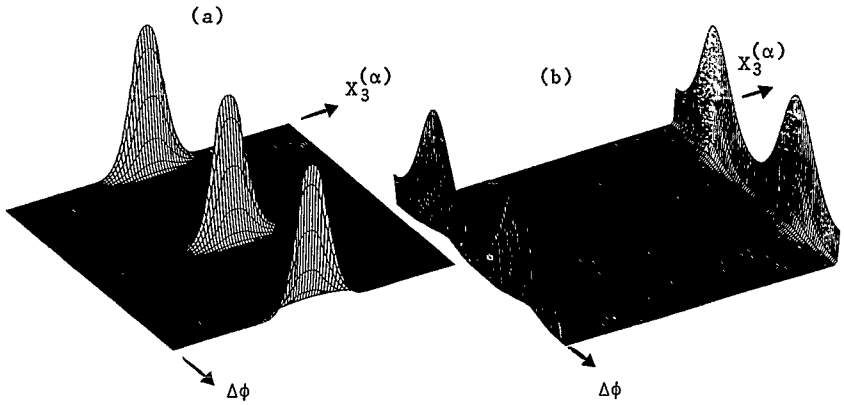

Figure 4 : Phase-space distribution functions $(-\alpha<X_3^{(\alpha)}<\alpha, -\pi<\Delta\varphi<\pi)$:
(a) Rotational (n=89,K=0,M=0) state
(b) Vibrational (n=89,K=88,M=0) state

5. STATISTICAL PROPERTIES OF THE ENERGY SPECTRUM

In the classically regular regime (Fig. 2a), there are only level crossings, or very small avoided crossings not visible at this scale, when inter-n-mixing takes place. This clearly follows from the fact that the different eigenstates are localized (see Fig. 1) near the invariant tori of the classical motion in phase space. Hence, two different eigenstates are localized in different regions and the energy levels cross.

When classical chaos appears, the energy levels anticross (right part of Fig. 2b and Fig. 2c). This is associated with the destruction of the phase-space invariant tori, leading to delocalization of the eigenstates and strong repulsion between them. Actually, the eigenstates associated with the motion close to the separatrix are the first ones to experience delocalization and strong anticrossings (see Fig. 2b).

As the magnetic field strength is increased, more and more energy levels anticross, which corresponds to the increasing size of chaotic regions (see Fig. 2c). Finally, above $\beta = 60$, all the energy levels do anticross (Fig. 2d).

The diagrams in Fig. 2 give a qualitative characterization of quantum chaos, that is, evolution from level quasi-crossing to level anticrossing when chaos develops. A quantitative measure is provided with the analysis of the statistical properties of the energy levels. It has been numerically shown that,

in the regular regime, these statistical properties are well described by a model of non-interacting eigenstates while, in the chaotic regime, they obey a random matrix model (here, the Gaussian Orthogonal Ensemble, see [15,23,24]).

However, such a generic random matrix model cannot explain any property of an hamiltonian system. Indeed, non-generic properties of the system still exist, such as phase-space localization of the eigenstates.

6. PHASE SPACE LOCALIZATION - SCARS OF SYMMETRIES

In the chaotic regime, the wavefunctions do not present any clear localization. Actually, especially for highly excited states, they fail to properly exhibit the dynamical correlations which still underlie the dynamics of the system. The phase-space distribution functions directly highlight these correlations (Fig. 3 and 4). We calculate some of them for "chaotic" eigenstates of the system in the strong field conditions of Fig. 2d. We choose a typical rotational state and a typical vibrational state. The phase-space distributions are plotted in Fig. 5. They are normalized with respect to the classical phase-space volume, that is, they should be constant for an "ergodic" eigenstate. This is clearly not the case. Figure 5a is localized near the classical fixed point ($X_3^{(\alpha)} = 0$, $\Delta\varphi = 0$). Such a plot is not very different from the one for a "regular" rotational state (compare with Fig. 4a). This indicates that the phase-space distribution function is strongly scarred by the rotational symmetry. The same feature is obtained for the "chaotic" vibrational state (Fig. 5b to compare with Fig. 4b) which phase-space distribution function is localized near $X_3^{(\alpha)} = \pm\,\alpha$ and scarred by the vibrational symmetry. On the other hand, many "chaotic" phase-space distribution functions are not clearly localized.

Actually, the phase space localization manifests the existence of scars of the rotational or vibrational symmetries. By "scars", we mean that some localization still exists for the system in the chaotic region, in contradiction with Random Matrix Theories expectations [25]. In that sense, these scars are comparable to the scars found by Heller [26] in the wavefunctions of billiards, leading to weak and unexpected spatial localization effects.

These scars of symmetries have very important experimental consequences illustrated on the simulated spectra in Fig. 6 [27].

In Fig. 6a, we plot, for each eigenstate, a stick which height represents the amount of rotational symmetry (i.e. the projection of the eigenstate onto the subspace spanned by the pure hydrogenic rotational states). When the classical motion is regular (below -29cm^{-1}), the highest state of each hydrogenic manifold is strongly dominant, the other ones having nearly zero "rotational part".

When the classical motion turns chaotic, the rotational symmetry partly breaks down, leading to clusters of dominant states, approximately equally

spaced, but with no regular structure inside the cluster. The cluster spacing at E=0 is 1.5 $\hbar\omega_c$, corresponding to the usual Quasi-Landau resonances [1].

Figure 6b is a simulation of a real spectrum using optical excitation from the (2p,M=-1) state (which are the experimental conditions of [4]). The clusters of rotational levels are still visible, though very weakened.

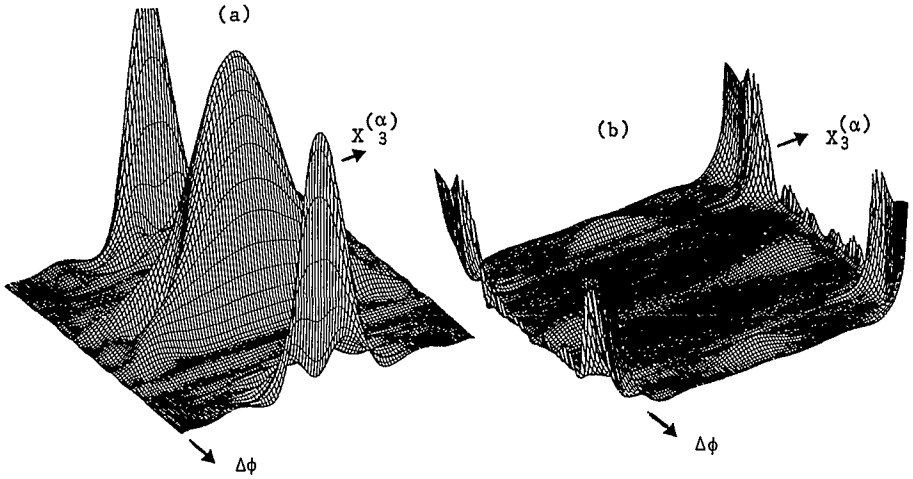

Figure 5 : Phase-space distribution functions for some "chaotic" eigenstates, represented in the $(-\alpha<X_3^{(\alpha)}<\alpha, -\pi<\Delta\varphi<\pi)$ plane.

(a) Rotational state
(b) Vibrational state

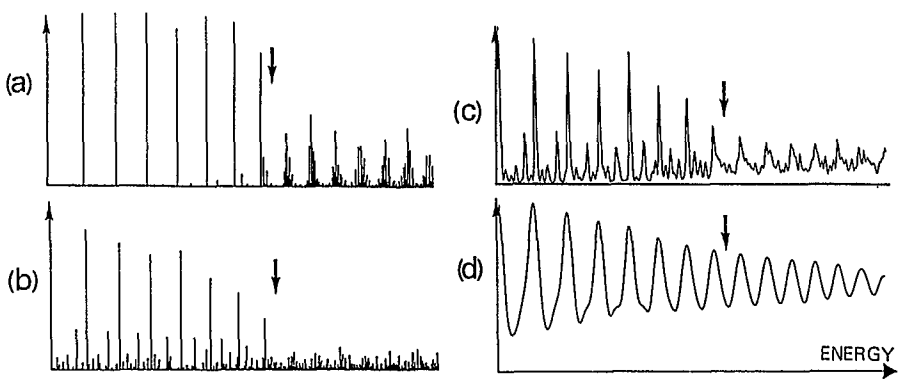

Figure 6 : Simulation of the M = 0, even parity spectrum of the hydrogen atom in a field of 8T between - 132 and 44 cm^{-1}

The arrow indicates the transition to complete chaos (-29 cm^{-1})

(a) Squared projections onto the rotational subspace
(b) Oscillator strengths from the (2p, M = -1) state
(c) Same than (b), with a resolution 0.5 cm^{-1}
(d) Same than (b), with a resolution 2 cm^{-1}

The symmetry of optical excitation is essentially spherical and does not comply with the internal symmetries of the magnetized atom : all the eigenstates are then efficiently optically excited. However, depending on the polarization being used, the intensities of the rotational or vibrational states may be favoured. With σ^+ polarization as used in Fig. 6b, the rotational states are preferably excited, which explains that the rotational clusters are visible. Figure 6c is a simulation of an experimental spectrum assuming finite resolution (modelled through convolution with a gaussian curve). The short-range fluctuations are partly smoothed out. At last, when a poor resolution is used (Fig. 6d), the spectrum looks "regular" continuously from the regular to the chaotic regime. The familiar aspect of the Quasi-Landau spectra with 1.5 $\hbar\omega_c$ spacing is rediscovered [1].

7. CONCLUSION

In summary, we have proved that the classically chaotic magnetized hydrogen atom has the following quantum characteristics :

* The short range fluctuations of the energy levels and eigenstates are essentially governed by a random matrix model.

* The long range behaviour traduces the essential part of the dynamics. At large scale, the spectrum is partly ordered : averaged over several states, the physical properties are regular and even present some periodicity. This is why low resolution experiments have shown regular features for a long time, and why high resolution experimental results are so difficult to interpret.

* The "fully chaotic" eigenstates of the quantum system are strongly scarred by the remnants of the low field symmetries, though the classical system is nearly completely chaotic and probably ergodic. These scars affect the phase-space distribution functions, expressing the internal dynamical correlations. Optical spectra reveal the existence of these scars, but the effects are weakened and entangled as optical excitation is a process not complying with the internal symmetries of the system.

REFERENCES

1. W.R.S.Garton and F.S.Tomkins, Astrophys.J. 158, 839 (1969)
2. J.C.Gay in "Atoms in unusual situations" Ed. J.P.Briand, Plenum (1986)
3. P.Cacciani, E.Luc-Koenig, J.Pinard, C.Thomas and S.Liberman, Phys.Rev.Lett. 56, 1124 (1986)
4. A.Holle, G.Wiesbuch, J.Main, H.Rottke, B.Hager and K.H.Welge, Phys.Rev.Lett. 56, 2594 (1986)

A.Holle, J.Main, G.Wiesbuch, H.Rottke and K.H.Welge, Phys.Rev.Lett. 61, 161 (1988)

5. O.Bohigas and M.J.Gianonni, in Lecture Notes in Physics 209 (1984) Springer-Verlag
6. T.H.Seligman, J.J.M.Verbaarschot and M.R.Zirnbauer, Phys.Rev.Lett. 53, 215 (1984)
7. T.Zimmerman, H.D.Meyer, H.Koppel, L.S.Cederbaum, Phys.Rev.A 33, 4334 (1986)
8. M.Gutzwiller, Phys.Rev.Lett., 45, 150 (1980)
9. If the (dynamical) symmetries are compatible, the system is regular whatever the field strength. A non-trivial exemple of such a system is the hydrogen atom in an electric field where the modified Runge-Lenz vector is a constant associated with the separability in parabolic coordinates
10. M.Henon in "Chaotic behaviour of deterministic systems", Les Houches Summer School (1983) North-Holland
11. M.J.Englefield, "Group theory and the Coulomb problem", Ed. Wiley, New-York (1972)
12. D.Delande and J.C.Gay, J.Phys.B Lett. 17, L335 (1984)
13. J.C.Gay and D.Delande in "Atomic excitation and recombination in external fields" Ed. M.H.Nayfeh and C.W.Clark, Gordon Breach (1985)
14. D.Delande, These de Doctorat d'Etat, Paris, unpublished (1988)
15. D.Delande and J.C.Gay, Phys.Rev.Lett., 57, 2006 (1986)
16. D.Delande and J.C.Gay, J.Phys.B Lett. 19, L173 (1986)
    D.Delande and J.C.Gay, Comm.At.Mol.Phys. 19, 35 (1986)
17. C.W.Clark and K.T.Taylor, J.Phys.B, 15, 1175 (1982)
18. D.Wintgen and H.Friedrich, J Phys.B 19, 991 (1986)
    D.Wintgen and H.Friedrich, J Phys.B 19, 1261 (1986)
19. D.R.Herrick, Phys.Rev.A 26, 323 (1982)
20. E.A.Solov'ev, JETP Lett., 34, 265 (1981)
21. M.V.Berry in "Chaotic behaviour of deterministic systems", Les Houches Summer School (1983) North-Holland
22. M.Hillery, R.F.O'Connell, M.O.Scully and E.P.Wigner, Physics Reports 106, 121 (1984)
23. D.Wintgen and H.Friedrich, Phys.Rev.Lett., 57, 571 (1986)
24. G.Wunner, U.Woelk, I.Zech, G.Zeller, T.Ertl, P.Geyer, W.Schweitzer and H.Ruder, Phys.Rev.Lett., 57, 3261 (1986)
25. D.Delande and J.C.Gay, in "Atomic excitation and recombination in external fields II", Ed. M.H.Nayfeh, C.W.Clark and K.T.Taylor, Plenum (1988)
26. E.J.Heller, Phys.Rev.Lett., 16, 1515 (1984)
27. D.Delande and J.C.Gay, Phys.Rev.Lett., 59, 1809 (1987)